

ENGINE DESIGN FOR A HALF SCALE MODEL OF JSF UAV WITH HIGH POWER EXTRACTION REQUIREMENTS

Cihat Akın¹, Coşku Çatorı²
TUSAŞ Engine Industries Inc.
Eskişehir, Turkey

Oğuz Eren³
Kale Aviation Industries Inc.
Istanbul, Turkey

Burak Özkahya⁴
TUSAŞ Engine Industries Inc.
Eskişehir, Turkey

Onur Tunçer⁵
Istanbul Technical University
Istanbul, Turkey

ABSTRACT

Unmanned aerial vehicles (UAV) are the future of air combat. These platforms have generic needs in contrast to manned air platforms. These needs should also be addressed from the engine design perspective. In this study conceptual design for a half-scale UAV (based on the dimensions of the Joint Strike Fighter) is presented. For this purpose a twin spool low by-pass ratio turbofan engine is designed. The main requirement is the high power extraction capability from the engine. This issue is addressed utilizing a novel alternator concept that relies on integrating the stator and the rotor on counter rotating spools. Furthermore on and off design point analyses and component design summaries are also presented. Outcome of the conceptual design task pushes the boundaries of the current state-of-the-art.

INTRODUCTION

UAV's remove the human limitations, human factor and offer more precise results. The future of air combat shall be dependent upon unmanned aerial vehicles without a shadow of doubt. Typically UAVs are equipped with a number of on board electronics with high power demand. However, current technology requires different solutions to the problem of on board electric generation. TJ-1 is designed to offer a possible solution to this problem. Despite their small size their electrical power requirement rivals that of conventionally piloted aircraft. From this standpoint a generic aero-engine design is needed in order to address this issue without the necessity of undesired trade-offs regarding aircraft performance (e.g. speed and maneuverability). This paper addresses such a design initiative.

The design task is initiated as per the requirements of a request for proposals (RFP) document which is published by AIAA for Undergraduate Engine Design Competition [1]. Designed system needs to deliver 67 hp of auxiliary power under all flight conditions. An additional 300 hp shall be required throughout the mission for avionics and weaponry, except for take-off and during combat maneuvers, which can occur at both subsonic and supersonic segments. This secondary power demand can be met via either the HP or the LP spool or some combination of both. As a secondary objective, maximum power extractable and how this is split is made between the spools without compromising the aircraft performance must be determined under two distinct mission conditions, which are 0,9 Mach at 35,000 feet and 1,4 Mach at 35,000 feet respectively.

¹ R&D Engineer, Email: cihat.akin@tei.com.tr

² R&D Engineer, Email: cosku.catori@tei.com.tr

³ R&D Engineer, Email: oguzeren@kale.com.tr

⁴ R&D Engineer, Email: basarburak.ozkahya@tei.com.tr

⁵ Associate Professor, Email: tuncero@itu.edu.tr

Design process should be carried out by taking into account two additional objectives. First one is aerodynamic similarity, which must be maintained with respect to the baseline engine model (F100-PW-229) by controlling the rotational speed of the spools. Second one is the minimization of fuel consumption considering the cost and logistics of military operation.

The design approach is as follows; first a parametric cycle analysis is performed regarding on and off design point requirements as per the RFP document, then component design issues are addressed one by one.

TECHNOLOGICAL STANDPOINT

First step in the design task is to form a database of existing concepts in order to grasp the technological and economical limits of the requested design. A study of F-135-PW-100, F-125-GA-100, EJ200 Mk.100 engines in addition to the baseline engine, provides useful reference points. General specifications of these engines are given in Table 1.

Table 1: Similar Engine Specifications

	F100-PW-229A		EJ200-Mk.100		F135-PW-100		F125-GA-100	
	Dry	Wet	Dry	Wet	Dry	Wet	Dry	Wet
Thrust (kN)	79	129	60	89	125	191	28	41
TSFC(g/kNs)	22.235	47.218	20.564	54.102	19.828	55.235	22.235	58.350
Airflow (kg/s)	115		74		91		42	
OPR	32		26		28		21	
By-pass ratio	0.36		0.4		0.57		0.49	
Compressors	3L,10H		3L, 5H		3L, 6H		3L, 4H + 1C	
Turbines	2H, 2L		1H, 1L		1H, 1L		1H, 1L	
Diameter (m)	1.2		-		1.3		0.6	
Length (m)	4.9		4.0		5.6		3.6	
Weight (kg)	1696		989		1701		617	

MISSION AND CONSTRAINT ANALYSES

A representative mission profile is defined for the UAV. Based on this profile mission and constraint analyses are carried out. Results of the constraint analysis are summarized in Figure 1. This graph shows the design point within the feasible domain and also provides comparison with respect to some existing aircraft. Mission analysis is conducted in order to calculate fuel requirements. For each mission leg weight fractions and fuel quantities are calculated. Results are demonstrated in Figure 2. As the engine parameters are dependent upon all these parameters this procedure is re-iterated until convergence.

PARAMETRIC CYCLE ANALYSIS

Turbomachinery cycle analysis consists of two different phases. First phase is called "parametric cycle analysis" which is developed in order to understand performance characteristic of the engine with respect to its design point. Parametric cycle analysis is a zero dimensional design, each module is represented with the associated change in the flow conditions. For example a compressor is defined with its compression ratio, its geometry is not defined at this stage. This preliminary stage is also referred to as rubber engine design. Because each point in the performance curve may correspond to a different physical engine. Parametric cycle analysis is performed to evaluate the inter-relationship between engineering choices, trade-offs and design constraints. This is also the pre-requisite for the off-design calculations. Off-design cycle analysis is conducted in the means of acquiring the performance characteristics of a physically defined engine in various flight conditions.

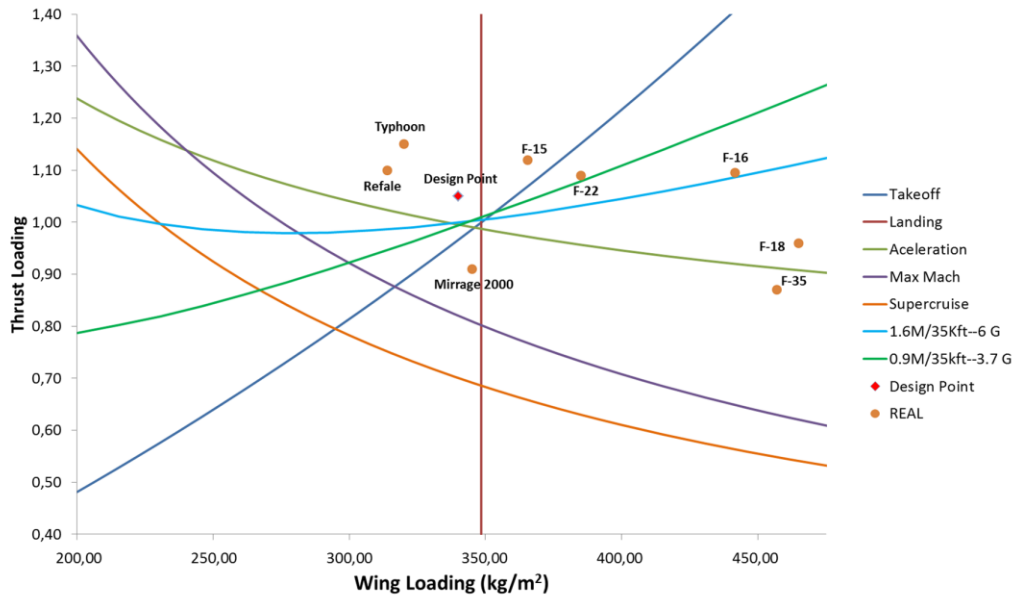


Figure 1: Constraint Analysis Results and the Selected Design Point

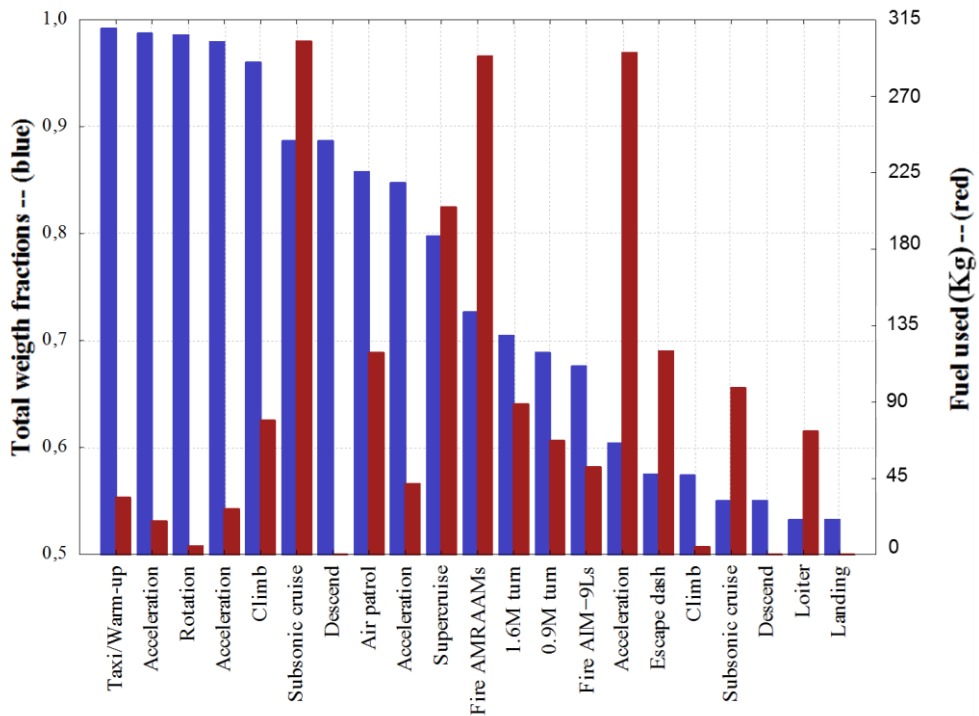


Figure 2: TJ-1 Weight Fractions and Fuel Used Throughout the Mission

Complete definition of the two spool low-bypass mixed turbofan engine with afterburner can only be concluded after the determination of a number of engine design variables, which are categorically summarized in Table 2.

Table 2: Engine Design Variables

Aircraft system parameter	$\beta, P_{TOL}, P_{TOH}, \epsilon_1, \epsilon_2$
Design limitations	h_{fuel}
Polytropic efficiencies	$e_f, e_{cL}, e_{cH}, e_{tH}, e_{tL}$
Component performances	$\eta_{burner}, \eta_{AB}, \eta_{mL}, \eta_{mH}$
Total pressure losses	$\pi_{intake}, \pi_{M,max}, \pi_{AB}, \pi_{nozzle}, \pi_{burner}$
Design choices	$\dot{m}, \pi_f, \pi_{cL}, \pi_{cH}, \alpha, T_{t4}, T_{t7}, M_{mix}, A_8/A_9, \theta_{break}, Alt_{design}$

Determination of these quantities is a non-trivial task. If these parameters are not chosen appropriately, non-realistic results may arise. Accurate usage of historical data and trends reduces the number of unknown design parameters, which is essential, given the number of unknowns.

While extracting power is the primary object of the design, conducting the exploration of the promising cycle boundaries under 67 hp continuous power load is found reasonable. Lastly, cooling air percentages have been taken same with baseline values until actual values are calculated at turbine design stage. This reflects the iterative nature of the design.

Three important unknown parameters for the engine are; θ_{break} , by-pass ratio and overall pressure ratio. Overall pressure ratio of a low bypass turbo fan engine defined by the fan and HPC pressure ratios. Nevertheless, choosing total pressure ratio and the compression ratio generated by the fan and the HPC as a design variable has great advantages considering evaluation and comparison of design alternatives.

Total pressure ratio is limited by the temperatures at the last stages of HPC, and it is usually between 35 and 45. However, it should be noted that increasing total compression ratio translates into an increment in length, weight and number of stage. It should however be noted that overall pressure ratio is not quite independent from the other parameters. Its value predominantly depends on the compressor design and the engine dimensions. Considering fuel consumption and engine dimensions, this value is limited within a certain range. Using historical trends, it would not be a bad estimate for this ratio to lie between 26 and 30. Therefore, overall pressure ratio is chosen to be 28 in the current design.

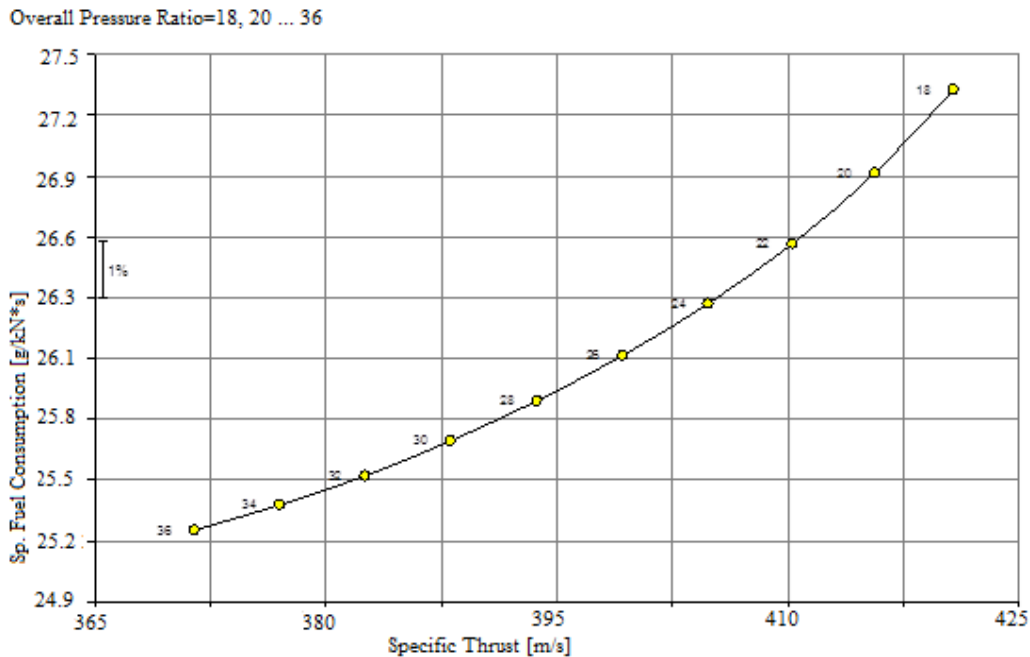


Figure 3: Overall Pressure Ratio (dry configuration)

By-pass ratio is the ratio between the mass flow-rate of the stream flowing into by-pass duct to mass flow rate into the core engine. Low by-pass ratio engines are a hybrid of turbojet and high by-pass ratio engines. By-pass ratio determines to which side it stands closer. As the by-pass ratio increases fuel

efficiency is improved. Decreasing the by-pass ratio increases specific thrust. Therefore, there exists a trade-off between the performance metrics.

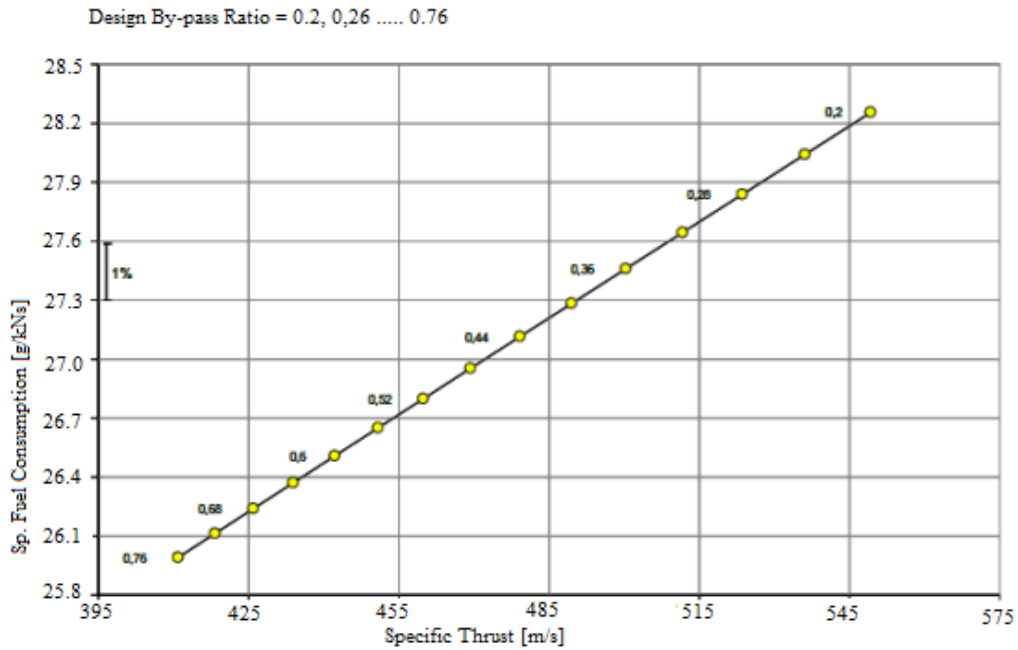


Figure 4: Design By-Pass Ratio (dry configuration)

While the engine is operating in non-augmented mode, increment in by-pass ratio leads to better fuel consumption yet worse specific thrust. One percent loss in specific thrust equals to a three fold reduction in fuel consumption.

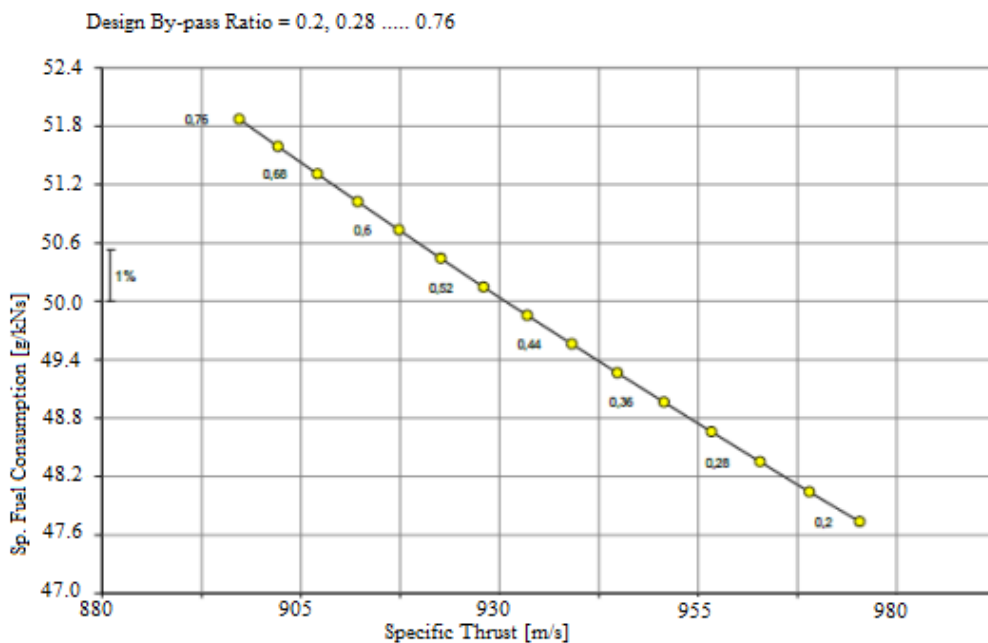


Figure 5: Design By-Pass Ratio (wet configuration)

While the afterburner is lit however, an increment in the by-pass ratio negatively effects both the fuel consumption and the thrust generation. Ratio of percentage rise in the fuel consumption and decline in the specific thrust equals to 0.9. This would be a negative ramification of opting for a high by-pass ratio. These two opposite trends turns selecting the correct by-pass ratio into a more challenging task.

A proper cycle selection cannot be made without considering fuel consumption. Therefore off-design data, acquired from all combinations of θ_{break} and by-pass ratios are used to determine the coefficients appearing in TSFC and thrust lapse correlations for mission profile calculations. In order to remove the negative effects of other design parameters (fan pressure ratio, mixer Mach number, core/by-pass pressure ratio) need to be taken into account. Furthermore, in order to make proper design choices a sensitivity analysis is conducted. Results are summarized in Table 3.

Table 3: Sensitivity Analysis Results

	Range	Afterburner Off		Afterburner On	
		TSFC (g/kNs)	Specific Thrust (m/s)	TSFC (g/kNs)	Specific Thrust (m/s)
Temperatures (K)					
Turbine Inlet Temperature	1445-1945	2.294	0.135	-0.219	0.062
Reheat Temperature	1445-1945	-	-	0.200	0.062
Pressures					
Overall Pressure Ratio	18-36	-2.323	-0.029	-0.026	0.006
Inner/Outer Fan Pressure Ratio	1.04-1.28	-0.085	0.004	-0.047	0.014
By-pass/Core Pressure Ratio	0.60-1.32	0.736	0.011	0.031	0.009
By-pass					
By-pass Ratio	0.20-0.76	-2.153	-0.008	0.077	-0.026
Mixer Mach Number	0.10-0.30	0.028	0.000	0.047	-0.014

Design Mach number and altitude are the most important parameters that determine the off-design performance of the engine. Design reaches its peak turbine inlet temperature and compression ratio simultaneously at its pre-determined design point. How these two variables affect the engine is determined by investigating the non-dimensional temperature theta break (θ_{break}). Engine performance is limited by the compression ratio P_3/P_2 before θ_{break} , after the design point however maximum turbine inlet temperature T_{t4max} shall start to limit the engine.

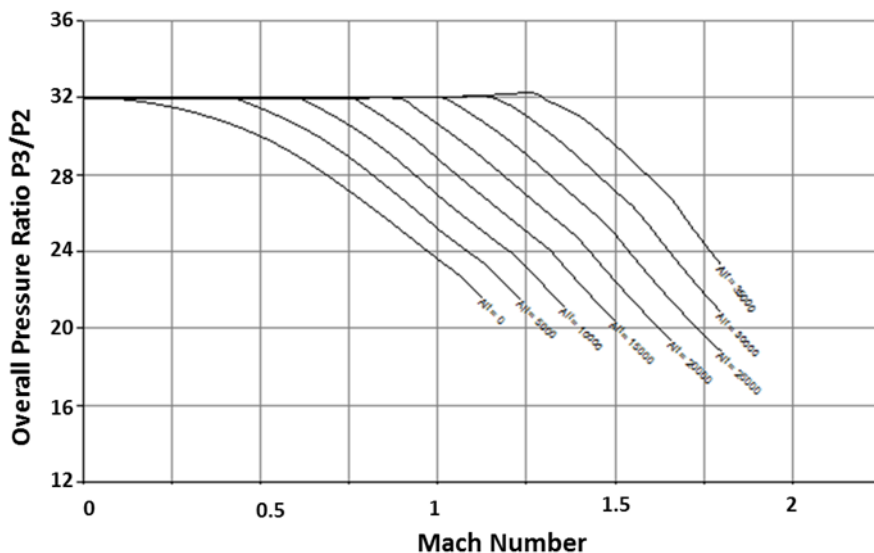


Figure 6: Total Pressure Ratio in Flight

Relationship between the altitude and θ_{break} is linear and weak; meanwhile the relationship between the altitude and the Mach number is strong and parabolic. Consequently, design calculations are carried out at the sea level. After setting the design altitude at the sea level, the design Mach number is left as the only variable affecting θ_{break} . Two important goals are set in the design. First one was to minimize fuel consumption with dry configuration. Other criterion was to maximize thrust generation with wet configuration (afterburner on). Therefore, the effect of θ_{break} on the engine is investigated using these two criteria.

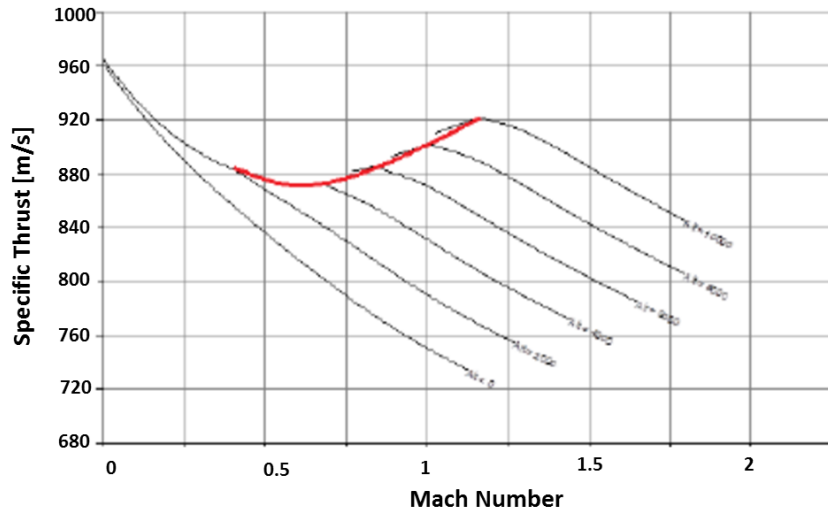


Figure 7: Specific Thrust in Flight ($M_{crit} = 0$, $Alt_{design} = 0$ ft, $\theta_{break} = 1$)

In Figure 7, specific thrust graphic with wet configuration can be seen. Here θ_{break} values are marked with red lines. Note that θ_{break} at this configuration is set to unity. Breaking points from the line trends can easily be seen in the figure. These points are the θ_{break} values for the engine. Here important thing to notice is the negative slope of the line. This requires θ_{break} to be higher than unity and chosen as 1.1 in order to reduce the thrust loss at high Mach numbers.

The choice of by-pass ratio and θ_{break} respect to engine airflow requirement for requested thrust values at RFP at wet condition is shown in Figure 8. The design point is marked on this figure is chosen also respect to the Figure 9 which defines the fuel efficiency of the engine.

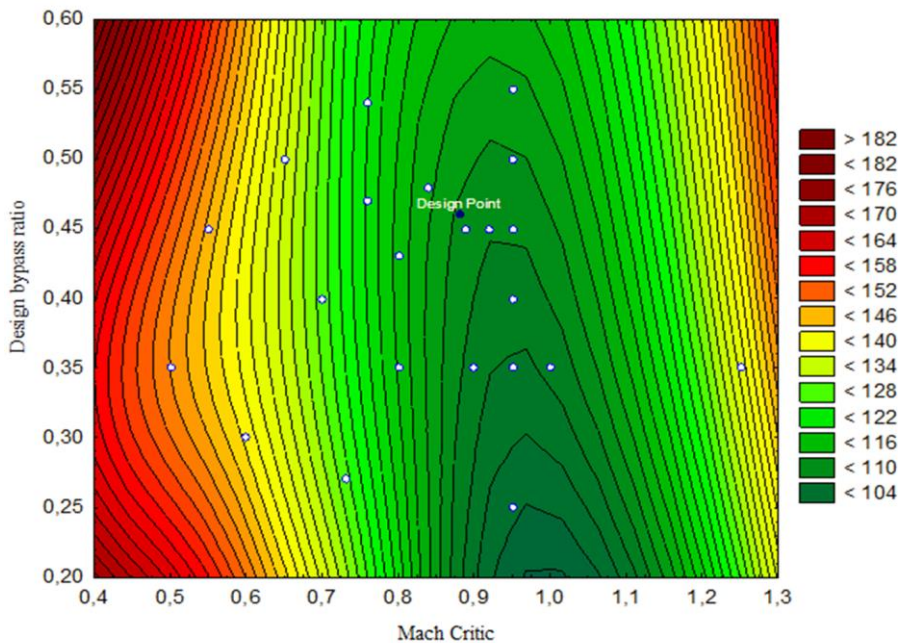


Figure 8: Airflow Requirements versus Flight Mach Number and By-Pass Ratio (Contours indicate airflow requirement in lbm/s)

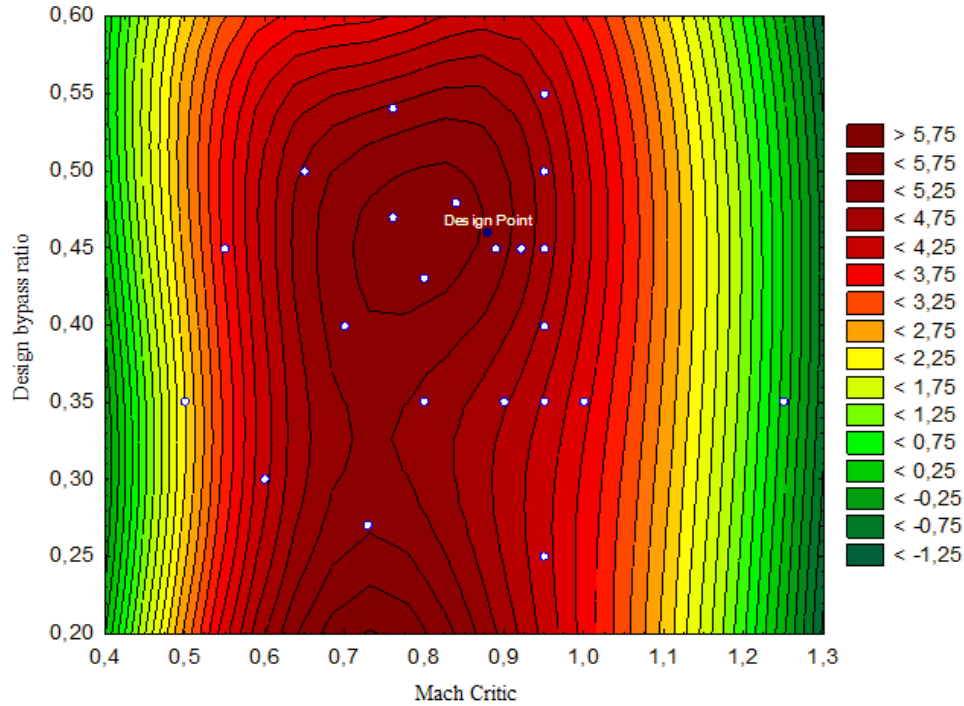


Figure 9: Percentage of fuel saved versus Flight Mach Number and By-Pass Ratio

There will be a thorough investigation for the remaining parameters. A proper selection cannot be made without considering fuel consumption. Therefore off-design data, acquired from all combinations of θ_{break} and by-pass ratios are used to determine the coefficients in TSFC and thrust lapse equations. In order to remove the negative effects of other design parameters (fan pressure ratio, mixer Mach number, core/by-pass pressure ratio) need to be taken into account. Engine design is optimized at Mach 1.4 and 35,000 ft altitude flight conditions. Design specifications of the aero-engine are summarized in Table 4. These numbers reflect a state-of-the-art engine design.

Table 4: Engine Design Specifications

Overall Pressure Ratio	28
Design Mach Number	1.1
Design Altitude	20,000 ft
Fan Pressure Ratio	4.15
LPC Pressure Ratio	3.59
HPC Pressure Ratio	7.99
Mixer Mach Number	0.25
Maximum Turbine Inlet Temperature	1667 K
Maximum Afterburner Inlet Temperature	1778 K

COMPONENT DESIGN

Inlet Design

Inlet shall be able to operate in both subsonic and supersonic regimes. In this context, note that it is preferable to keep compressor's axial speed constant from an efficiency point of view. Inlet transmits the air to compressor at a specific speed, independent from flight conditions. Inlets are designed to reduce the air speed to engines operable conditions while minimizing the pressure loss. In subsonic region, 1% of pressure loss in inlet approximately equals 1% loss in thrust generation. In supersonic region thrust loss increases non-linearly [2].

Engine is designed with a two dimensional variable ramp having two external oblique shocks. Two symmetrical ramps at each side of the A/C are proposed to be attached to engine with s-ducts in order to prevent fan face being hit by radio waves.

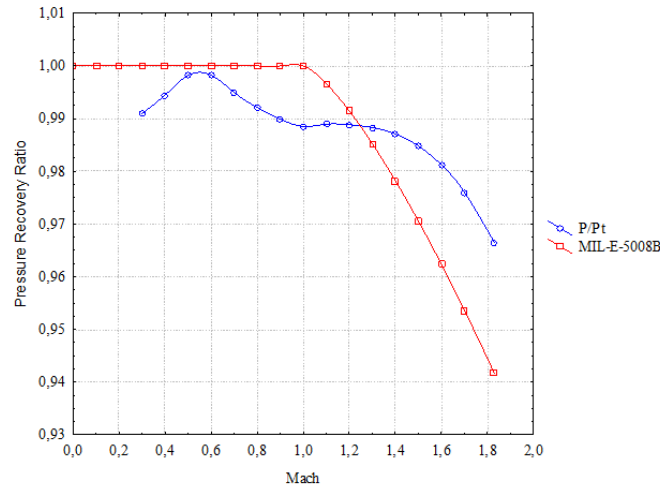


Figure 10: Inlet Pressure Recovery Ratio

Maximum required inlet area by the engine is 0.275 m^2 . There is a 4% of safety margin and boundary layer bleed requirements are included (0.8 at 0% and 1.8 at 4%, linearly varying). Isentropic flow equations are used for inlet design. In order to achieve maximum pressure recovery, a definition introduced by Oswatitsch is used [3]. Oswatitsch states that in a system with $n-1$ oblique shocks and one normal shock, maximum recovery is achieved when the oblique shocks have equal power. Total pressure recovery performance of the inlet given with MIL-E-5008B standard at Figure 10. Since the engine should be housed inside the fuselage, a Y-shaped inlet duct, whose dimensions are shown in Figure 11, this shape provides minimal pressure loss. A side view is also provided in Figure 12.

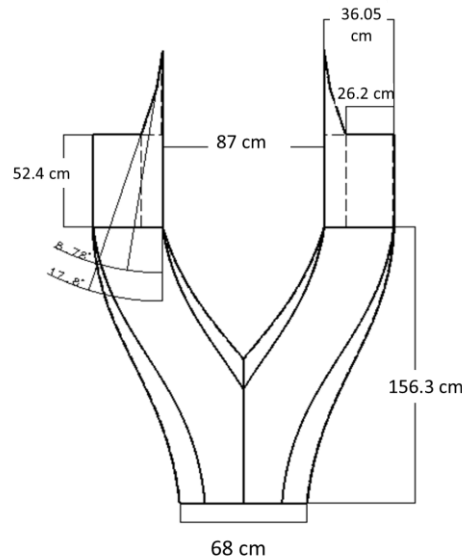


Figure 11: Inlet Dimensions

The designed two-ramp system has a fully variable geometry. For each and every Mach number, both ramps shall optimize their angles in order to maintain the best pressure recovery. As a safety margin, maximum Mach number is increased by 0.03 and taken as 1.83. Inlet geometries corresponding to 1.4 and 1.8 Mach numbers are provided in Table 5.

Table 5: Ramp Angles

	1.4 Mach	1.83 Mach
First shock angle	51.1	41.8
First ramp angle	4.0	8.8
Second shock angle	60.3	53.1
Second ramp angle	3.6	9.0



Figure 12: Inlet Geometry

At zero flight speed pressure recovery factor is calculated as 0.804, which falls within acceptable limits. Therefore, auxiliary air inlets should be incorporated into the design. Reverse calculations are made for $\eta_r = 0.95$ and Mach number at the throat is found as 0.285. Required extra auxiliary air inlet area for that Mach number is 0.26 m^2 . TJ-1 includes two identical inlets, thus dividing by two the resulting area has been found to be 0.13 m^2 . These auxiliary inlet doors shall ensure the desired pressure recovery.

Fan and Compressor Design

Request for proposals (RFP) demands a two spool low by-pass turbofan engine, however this does not mean only two compressors must be used. More than one compressor on a same shaft is also possible. For the current design, a centrifugal compressor is considered in lieu of the last four stages of the high pressure compressor. However, efficiency calculations show that efficiency of a centrifugal compressor shall be between 0.75 and 0.8. Although their tolerance to rapid flow rate change is lower, axial compressors are found the most suitable type considering its relatively high corrected flow rate and better efficiency.

For the high pressure compressor; a repeating row, repeating stage, mean line design, meanwhile for the fan; a constant tip radius, repeating row and repeating stage design approach has been found appropriate for preliminary calculations. The flow properties are assumed constant throughout the azimuthal and span-wise directions. Calculations are only performed for the mean line properties. Axial velocities are constant and air is assumed to be calorically perfect. Swirl angles are assumed to be constant along the stages. Free vortex swirl model is used for the conceptual design.

Blade tip Mach number is selected as 1.27 for the fan and 0.93 for the HPC respectively. These values are same as baseline engine's blade tip Mach numbers. This approach is followed in order to fulfill the requirement of using replica blades of the baseline engine [1]. It is clear that the blade tip Mach numbers are the first constraint for the compressor. Second one is the engine dimensions since this engine shall be mounted on a half scale model of JSF. Data from the parametric cycle analysis are used to determine the smallest possible dimensions for obtaining the necessary thrust. Blade and rim stresses must also be considered. These are strongly dependent on the compressor dimensions.

Table 6: Fan Design Summary

Number of stages	3
Mass flow rate (kg/s)	47.81
Rotor angular speed (rad/s)	1275
Inlet total pressure (kPa)	101.32
Inlet total temperature (K)	309.44
Entry angle (degrees)	31.60
Entry Mach number	0.60
Diffusion factor	0.55
Rotor chord/height ratio	0.59
Stator chord/height ratio	0.59
Polytropic efficiency	0.89
Solidity	1.10
Exit angle for the last stage	31.60
Exit Mach number for the last stage	0.48

Fan and high pressure compressor's RPM values have to be the same with the low and high pressure turbines respectively, since they are mounted on the same shaft. Therefore, turbines and compressors

are initially designed separately, but afterwards they are optimized together. This may decrease the turbine and compressor efficiencies individually, however overall efficiency is the important issue.

As the first step of the design process, stage counts are determined, paying attention to stage loading and flow coefficients. Considering the state-of-the-art, stage loading is limited to 0.7 [4] and flow coefficient varies from 0.45 to 0.55 [5]. Main goal of this process is to introduce the most efficient compressor design without exceeding limits and constraints.

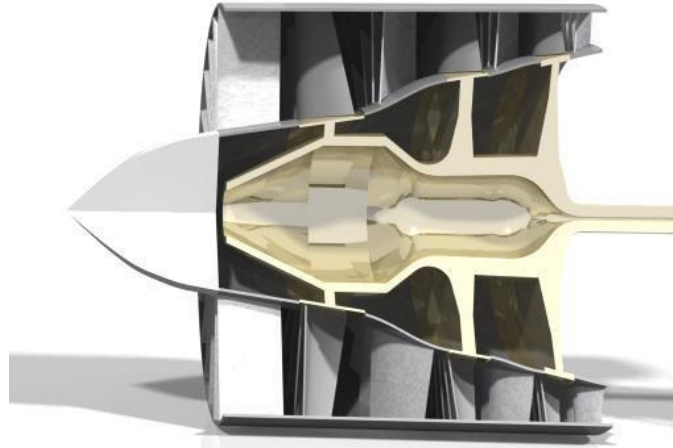


Figure 13: Cut-Away View of the Fan

High pressure compressor (HPC) design is carried out, using the same approximation and assumptions with a single difference. Mean line design is preferred since blade height is low relative to the mean radius. If the disc gets larger, disc bore stresses will also be higher. In order to avoid high stresses at the bore region, this type of design has been preferred.

Same design approach is repeated for the HPC. First, the stage count is determined from the total temperature rise and nine stages are found suitable. Additionally, polytropic efficiency, solidity and diffusion factor are assumed to be 0.89, 1.1 and 0.55 respectively. These values are almost at the limit of the current trends. Thus this conceptual design pushes towards the state-of-the-art limits.

Hub to tip ratio of the first stage is chosen to satisfy the given tip radius. RPM of the HPC only depends on the tip radius and the tip speed. Tip speed is found from the circumferential tip Mach number constraint. With the radius known, RPM is calculated easily. Throughout this process, HPC and HPT calculations are performed together. Since the HPT is more demanding because of high temperatures, compressor's tip radius is determined from required high pressure turbine RPM and radius. Aspect ratio of the compressor blades have to be same as the blades used in baseline model which is 2.7.

Table 7: HPC Design Summary

Number of stages	9
Mass flow rate (kg/s)	32.75
Rotor angular speed (rad/s)	1970
Inlet total pressure (kPa)	360.18
Inlet total temperature (K)	464.44
Entry angle (degrees)	29.4
Entry Mach number	0.47
Diffusion factor	0.55
Rotor chord/height ratio	0.37
Stator chord/height ratio	0.37
Polytropic efficiency	0.89
Solidity	1.10
Exit angle for the last stage	29.4
Exit Mach number for the last stage	0.33

Table 10: Air Partitioning ($T_g = 2318$ K, $\epsilon_{pZ} = 0.8$)

	Total	Primary Zone	Secondary Zone	Transpiration Cooling	Dilution Zone
Airflow (kg/s)	77.1	25.5	12.3	19.3	17
Mass Fractions	1.00	0.37	0.16	0.25	0.22

Swirler blades are chosen as airfoil cross-sections with 0.64 drag coefficient and 35° blade angle. After calculations, swirlers are arranged as in Figure 15. Swirl number is 0.61, which corresponds to a moderate swirl intensity.

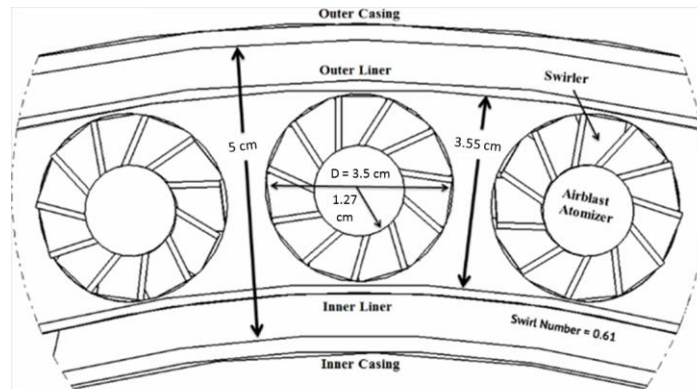


Figure 15: Swirler Layout

Afterburner radius is chosen as 0.35 meters, this value corresponds to the maximum diameter of the engine. Flow leaving the turbine is mixed with the by-pass stream prior to afterburner entrance. Combustion parameters for the combustor and the afterburner along with rule-of-thumb design guidelines are listed in Table 11.

Table 11: Combustion Parameters

	Burner	Design Guideline
Combustor Loading ($\text{kg/s} \cdot \text{atm}^{1.8} \cdot \text{m}^3$)	0.5	Max. 10
Combustion Intensity ($\text{MW}/\text{atm} \cdot \text{m}^3$)	30	Max. 60
	Afterburner	Design Guideline
Combustor Loading ($\text{kg/s} \cdot \text{atm}^{1.8} \cdot \text{m}^3$)	5.16	Max. 100
Mach Number	0.23	Max. 0.3

Turbine Design

Conventional turbine designs for flow rates greater than 13.6 kg/s are mostly axial turbines. Thus, design process begins with the decision of both high pressure turbine (HPT) and low pressure turbine (LPT) being axial type. In turbomachinery, there is never a best turbine design for a given application there exists always certain trade-offs between several parameters such as, rotor stress, weight, outside diameter, efficiency, noise, durability, and cost, such that the final design lies within acceptable limits for each parameter. The primary goal of the turbine design is to develop a turbine which shall meet the design requirements set forth in the parametric cycle analysis phase.

The expansion ratio of the turbines, the need of fewer stage numbers and the counter-rotating spool dynamics, led to a brand new design in spite of being a replica of the baseline engine. This choice reveals a bunch of challenges to be overcome in the design process. Challenges have been mainly categorized as structural and aerodynamic.

The structural limitations may be sub-categorized into; uncooled configuration of LPT, material and cooling limitations for the high rotational speeds of HPT. The aerodynamic limitations themselves may be further sub-categorized as; choking turbine rotor inlets while maintaining the subsonic flow over the

airfoil and correlating all these design decisions within the compressors' feasible operating RPM range. HPT and LPT specifications are selected in the ranges of open literature sources and research conducted by NASA.

The performance parameters for a turbomachine operating with compressible fluid mechanics, can be expressed as per Eq. 1.

$$\Delta h_{0s}, \eta, P = \mu, N, D, \dot{m}, \rho_{01}, a_{01}, \gamma \quad (1)$$

Further investigation of the isentropic relations between temperature and pressure, yield more useful non-dimensional functions that can be expressed as follows (Eq. 2). The first parameter at the right-hand side is the equivalent mass parameter (\dot{m}_{eq}) and the second one is the equivalent speed parameter (N_{eq}) where δ is the ratio of total pressure at the inlet to the US Standard Sea-Level Pressure and θ is the squared ratio of critical velocity at the turbine inlet to the US Standard Sea-Level critical velocity. The stage loading of this design is 1.94 and the expansion ratio is 3.44.

$$\frac{P_{02}}{P_{01}}, \eta, \frac{\Delta T_0}{T_{01}} = f \left(\frac{\dot{m}\sqrt{\theta}}{\delta}, \frac{N}{\sqrt{\theta}} \right) \quad (2)$$

Since it is impossible to generate a single-stage turbine design based on the baseline engine, replication blades, as suggest in RFP [1], have been ruled out. A new approach will be investigated to obtain the cycle analysis parameters listed in Table 12.

Table 12: HPT Design Point Parameters (1.1 M, 20 kft)

Total Enthalpy Ratio	0.78
Total Pressure Ratio	0.30
Mass Flow Rate, kg/s	30.9
Rotational Speed, rpm	18812
Inlet Total Pressure, kPa	2709.6
Inlet Total Temperature, K	1666.7

A half-size JSF shall be mounted with the designed engine. According to Raymer correlations [6] the design length of the engine will approximately be 3.6 m. Therefore, a tradeoff study should be performed to check whether it is better to design a single-stage turbine, while pushing the design limits, or to design a two-stage turbine, as it is in the baseline engine F100-PW110-229. A simple comparison between these two designs is made via rough estimations. Multi-staged design offers lower centrifugal loading and higher efficiency, while single-stage design offers a large saving in the manufacturing cost, weight, and maintenance costs because of the significant reduction in the number of components, especially expensive cooled airfoils. Considering the comparative advantages of each design, a single-stage design is found adequate and appropriate.

In this study, a NASA report [7] is used as a baseline. In the report, a single-stage uncooled turbine design, which has a rim speed higher than the suggested values in the literature, is tested in a cold air rig. The design and test parameters are provided in Table 13.

Table 13. Conditions of Cold Air Rig Test of a Single-Stage Turbine at NASA (Moffit, 1980)

Performance Parameter	Design Condition	Test Condition
Inlet total temperature, K	2200	288
Inlet total pressure, N/cm ²	560	10.1
Mass flow rate, kg/s	49.4	3.9
Turbine rotational speed, rpm	21772	8081
Blade tip speed, m/s	579	705

In the NASA effort [7] designed turbine is validated by experiments while maintaining correlated aerodynamic and thermodynamic similarities. In Table 14, it can be clearly seen that there is a difference between the TJ-1 design values and the test values. This means, correlations are not enough to consolidate a direct application of the designed turbine to TJ-1. Further calculations and tests are needed to meet the parametric cycle analysis requirements. Furthermore, this not acceptable for an equivalent design for TJ-1, but it is enough to reveal the feasibility of the design.

Table 14. Performance Parameter Values

	Test Values	Design Values	TJ-1 Design Values
m_{eq} , kg/s	8.50	7.71	6.22
N_{eq} , rpm	8081	8066	7970

A mean-line design is conducted for the turbine using TURBN program developed by Mattingly [8]. Since it is not possible to provide comprehensive methods for turbine design, calculations are made under constant axial speed and adiabatic assumptions with selected relative Mach number constraints for the stator and rotor airfoils. Nevertheless, these conditions stated above are sufficient to analyze the turbine behavior. Analyses should reflect the engine cycle assumptions and resemble actual turbine designs.

Table 15: HPT Design Parameters

Stage Loading Coefficient	Flow Coefficient	Isentropic Efficiency	Aspect Ratio		Solidity		Number of Blades	
			Stator	Rotor	Stator	Rotor	Stator	Rotor
1.65	0.41	0.90	1	1.11	0.92	1.49	62	74

There are three parameters controlling the turbine efficiency; stage-loading coefficient, flow coefficient and the degree of reaction. From the Smith chart (Figure 16), uncooled total-to-total turbine efficiency (η_{tH}) is found to be 0.91.

After fixing the aerodynamic and thermodynamic design of the HPT, two significant issues remain. First, to be able to withstand the stresses generated. Secondly, to be able to operate for estimated working hours without material or mechanical failure.

In turbine structural analysis, the limiting factor would most likely be the creep behavior, especially for the turbines operating at high temperatures and high rotational speeds. TJ-1's HPT is subject to a higher creep risk due to its higher rotational speed. The centrifugal stress is directly proportional to the material density. Thus, a semi-iterative method should be followed while calculating the stresses and selecting the materials.

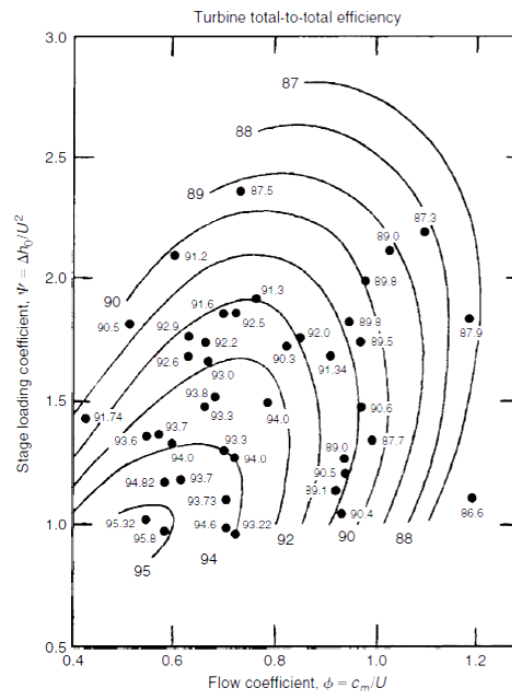


Figure 16: Smith Chart for Turbine Stage Efficiency (Dixon et.al., 2010)

For the rotor, the taper ratio (A_r/A_h) is selected within the recommended boundaries [8] as 0.7 in order to reduce the stress. The average annulus area (A_{av}) is 0.063 m^2 and the rotational speed ω is 1970 rad/s. Centrifugal stress σ_c is found as 259.9 MPa. SC 16 single crystal Nickel alloy has been chosen

for the nozzle guide vane (NGV) and the rotor blades of the HPT. SC-16 has 2000 hours creep rupture life at 850 °C for 275 MPa operating stress [9]. Oxidation and elongation performances are also taken into consideration in the material selection process.

For 74 rotor blades and 10% airfoil thickness, disk stress (σ_d) is found approximately 450 MPa for a disk shape factor (DSF) of 2.1. These stress levels are allowable by the selected material since the disk temperature is 100-200 °C lower than the blade average.

The cooling effectiveness Φ is 0.62 for 850 C material and 820 °C coolant flow temperatures. As stated by Hess in "Laminated turbine vane design" NASA report [7], with 6.17% coolant mass flux ratio and 0.62 cooling effectiveness, cooling from 1538 °C to 647 °C (mass average temperature) can be succeeded. Thus, in TJ-1 HPT, cooling mass flux ratio of 5% is found sufficient for the turbine rotor temperature to drop from 1355 °C to 850 °C. Nevertheless, NGVs are not exposed to high centrifugal stress that the rotors are, coolant percentages should be examined for distribution along the turbine for better engine performance. Further rotor creep rupture life can be procured by ceramic coating which provides a 400 °C temperature decrease on the airfoil surface. That means 1.2-1.3 times more rupture life than uncoated. However, a cost trade-off analysis should be done to improve average time between maintenance costs.

In LPT design, the same trade-off between one and two stage design is made once again. A one stage design is decided upon since the limiting boundaries are not tight. LPT design has a similar process with the HPT design, a mere difference is that the rotational speed is known as a limiting factor because of the fan's operating RPM, which is 1275 rad/s.

Table 17: LPT Design Point Parameters (1.1 M, 20 kft)

Total Enthalpy Ratio	0.85
Total Pressure Ratio	0.451
Mass Flow Rate, kg/s	33.47
Rotational Speed, rpm	12175
Inlet Total Pressure, kPa	813.6
Inlet Total Temperature, K	1255

Stage loading coefficient, flow coefficient and turbine reaction are stated in Table 18. Results are consistent with the limitations in the literature while providing an uncooled total-to-total 0.91 turbine polytropic efficiency.

Table 18: LPT Design Parameters

Stage Loading Coefficient	Flow Coefficient	Isentropic Efficiency	Aspect Ratio		Solidity		Number of Blades	
			Stator	Rotor	Stator	Rotor	Stator	Rotor
1.97	1.00	0.91	1	1	0.886	2.08	34	71

As it has been in HPT, the same structural assumptions and calculations have been made in LPT. The only difference is that LPT requires uncooled design. Parameters are either selected or calculated as follows; $A_t/A_h=0.7$, $A_{av}= 0.086 \text{ m}^2$, $\omega=1275 \text{ rad/s}$ and $\sigma_c=151.7 \text{ MPa}$. The same material which is used for HPT, SC-16 is also used for the LPT. Average total temperature at the on-design point is 950 °C. SC-16 has 1000 hours of creep rupture life for 150.03 MPa at 950 °C. This life is fairly low for a turbine design, but as it was explained in HPT design, a ceramic thermal coating shall drop the temperature of the blades by about 55-65 °C which gives three times more rupture life to the turbine. In conclusion, an uncooled LPT design is achievable at the design conditions.

Mixer Design

In mixer design, in order to keep the dimensions as small as possible, a mixer-diffuser design has been chosen. In addition, diffuser efficiency is chosen as 0.9 as it was stated in Mattingly, Heiser and Pratt (2002) for flat wall and dump diffuser's. Table 19 lists the general dimensions of diffuser, Figure 17 shows the layout.

	Station 6A	Station m	Station 6.1
R_{outer} (cm)	35	35	35
R_{inner} (cm)	20.93	27.96	0
R_{mean} (cm)	27.96	23.04	17.5
H (cm)	14.07	23.93	35
A (m ²)	0.247	0.346	0.374

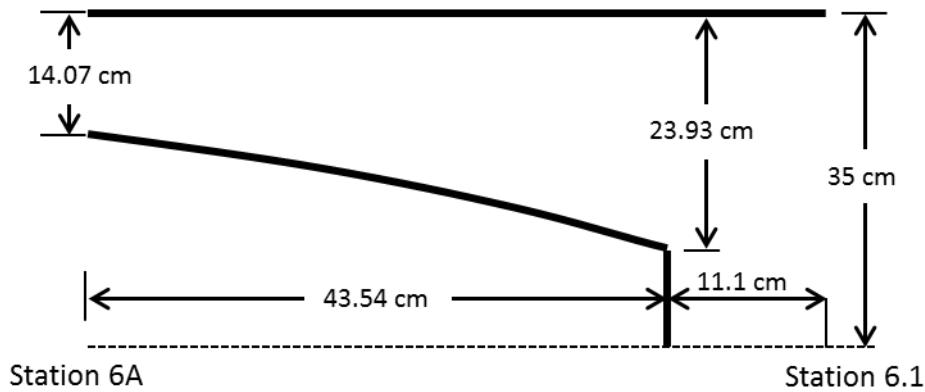


Figure 17: Mixer + Diffuser Layout

Nozzle Design

Nozzle has a strong effect on thrust and specific fuel consumption. Variable geometry nozzle design becomes prominent since can alter the operating conditions of the engine during off-design conditions.

Low corrected mass flow rates cause the operating line to approach towards the surge line. Increasing nozzle throat area balances the engine back pressure, and also through increasing the corrected mass flow rate, it shifts the operating line away from the surge line.

Engines with afterburners must have variable nozzle throat areas for the sake of proper back pressure control. Engine should be able to operate at both subsonic and supersonic flow regimes, which means completely different nozzle area ratios for the engine.

Variable area nozzle also enhances the start-up transient. Opening the nozzle exit area reduces the back pressure on the turbines, leading to increased expansion ratio, such that turbines generate more power at lower turbine inlet temperatures. Hence a smaller starter can be used to provide a lighter engine.

Over or under expansion may occur during operation. Over-expanded nozzles have more pressure losses than under-expanded nozzles. Thus some margin can be put to use in order to avoid over-expansion since slight under-expansion is tolerable.

Two dimensional (pitch only) thrust vectoring is employed for the present design case since it increases maneuverability and decreases SFC at certain flight points. Thrust augmentation up to 7% is possible with thrust vectoring.

Nozzle should have high performance at all the mission segments as required by tactical aircraft. Even though performance is quite important, production and maintenance costs are also need to be considered. For a tactical aircraft, cost and maintainability issues are less important than lack of performance. Tactical aircraft flying over Mach 1.5 require a convergent-divergent variable nozzle [6]. Furthermore, the mission varies greatly over different segments. Hence, optimizing the nozzle for two design points, like the geometrically scheduled nozzle design approach, since it does not maintain high performance, led geometrically scheduled nozzle option to be omitted amongst design choices.

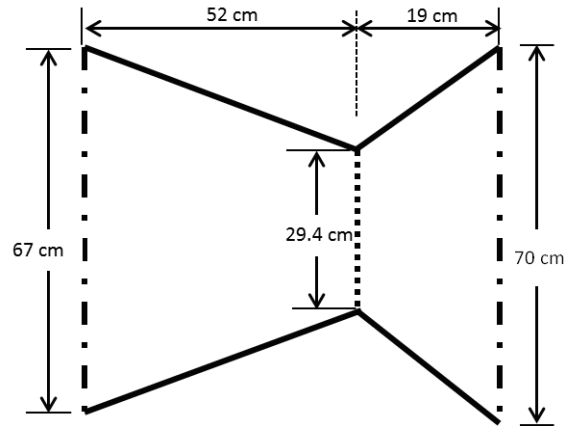


Figure 18: Nozzle Dimensions

Passively scheduled nozzle is also considered. This arrangement employs divergent section flaps which are allowed to move through a range for the same throat area. Internal pressure of the divergent section provides the necessary force to move these flaps through their range of possible area ratios [10]. Floating flaps is less complex. Therefore, light and floating flaps can fulfill the required performance. However there are some downfalls. This type of nozzle significantly reduces the region of flight envelope which aircraft operates at its off-design conditions [6]. Moreover, two dimensional thrust vectoring is not possible in the absence of full control over the divergent section. In the light of all these reasons fully variable nozzle has been found as the best solution for performance. Figure 18 depicts the nozzle dimensions of the TJ-1 engine.

Starter/Generator Design

Most aircraft use two separate systems for electric generation and engine start-up. Since weight is a strong factor which affects aircraft performance, a lighter engine will have a better performance under same circumstances. Combining these two systems saves weight as well as decreasing the total volume needed. This system type is called integral starter generator, and this approach is chosen for the current design.

RFP requires calculations for maximum power that can be taken-off at the following flight conditions; 1.4 M at 35000 ft and 0.9 M at 35000 ft altitude. Figures 19 and 20 show load shaft power requirement versus power offtake and the effect of load shaft power requirement on a number of operating variables (HPC and fan surge margins, net thrust, specific fuel consumption) respectively. Note that, using HP-spool for power extraction is more efficient than using LP-spool. However, in order to extract the maximum power without compromising the engine performance, power should be taken-off equally from both spools.

The starter/generator system, is placed within the engine hub, between the high and low pressure compressors. Main reason of this is to benefit from counter rotating shafts as much as possible. Additionally, a starter generator must be placed close to the HPC in order to eliminate the additional linkage elements since it cranks the HPC.

The system consists of two parts; first one is a 70 hp starter/generator switched reluctance machine whose stator is connected to the casing and rotor connected to the high-pressure spool. The second one is a 300 hp generator whose stator is connected to the high-pressure spool and stator is connected to the low-pressure spool. System can be seen in the Figure 21. Red shaft is the HPC spool and yellow one is the LPC spool. Pink and orange surfaces are the stator and the rotor of starter/generator (S/G) respectively. S/G's first responsibility is to provide 150 N.m constant torque on the HP-spool for starting the engine to 25% of its maximum speed (5000 RPM). The second responsibility of the S/G is to generate 67 hp for sub-systems throughout the mission and while the engine is at its idle condition.

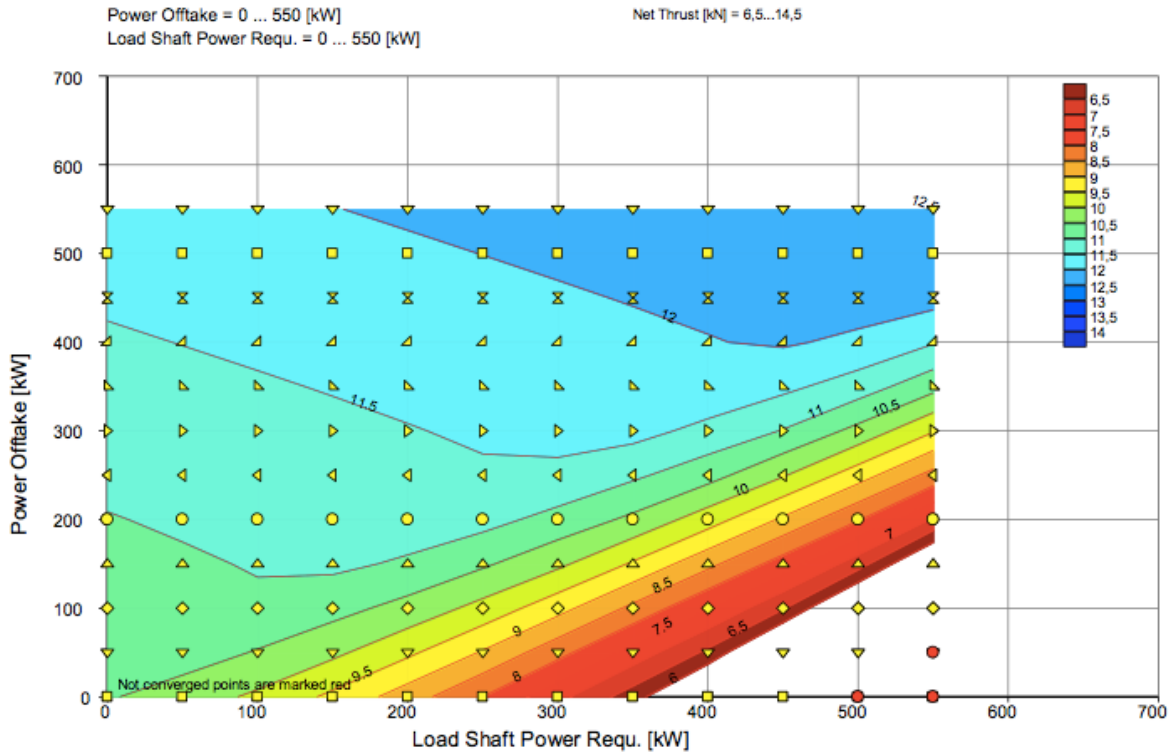


Figure 19: Load Shaft Power Requirement versus Power Offtake

Blue and brown surfaces indicate the stator and the rotor of a main variable frequency generator which provides 300 hp when needed. As one can see orange part is extend of high pressure spool in order to crank the HP-spool only. It avoids electromagnetic interaction with the LP-spool which offers better startup performance. The blue stator uses, the coils (indicated by brown color) which are attached to LP-spool, as its rotor. Thus, it favors the counter-rotating mechanism by obtaining 31500 relative RPM at full power and generates 300 hp from a compacter electrical generator. A converter circuit and a control program are necessary to manage the variable frequencies and shutting down the generator-only part for starting process.

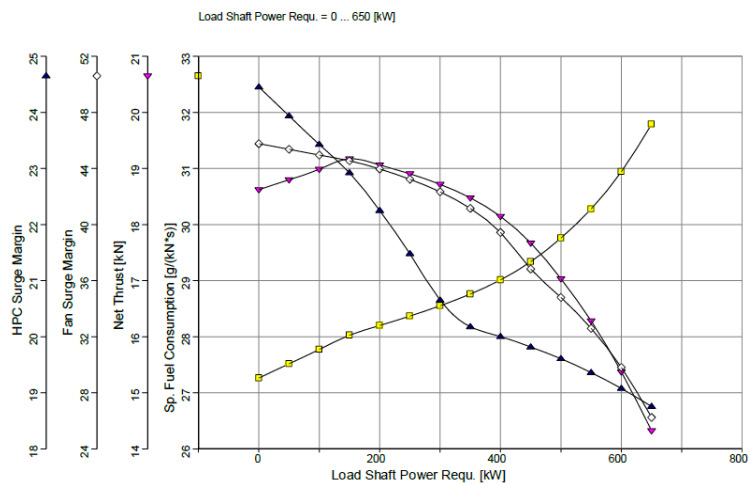


Figure 20: Power Extraction at Subsonic Cruise (0.9 M, 35 kft altitude)

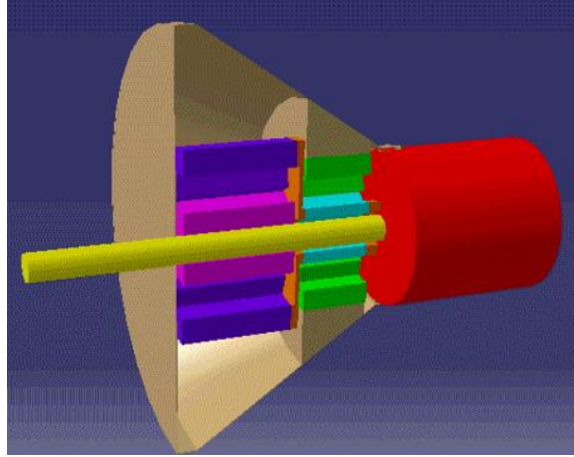


Figure 21: Conceptual Design of the Alternator

DISCUSSION AND CONCLUSION

An aeroengine conceptual design that meets the specifications outlined in the RFP document is accomplished. A cut-away view of the overall engine is presented in Figure 22. This engine represents a good compromise between the design requirements. Furthermore, TJ-1 incorporates a novel starter/generator design wherein the counter-rotating spools enable generation of 300 hp at full power within a compact unit. Consequently, the power requirement of the half scale (with respect to JSF) UAV is met. It is expected that these conceptual design ideas be utilized in practical system within the near future.

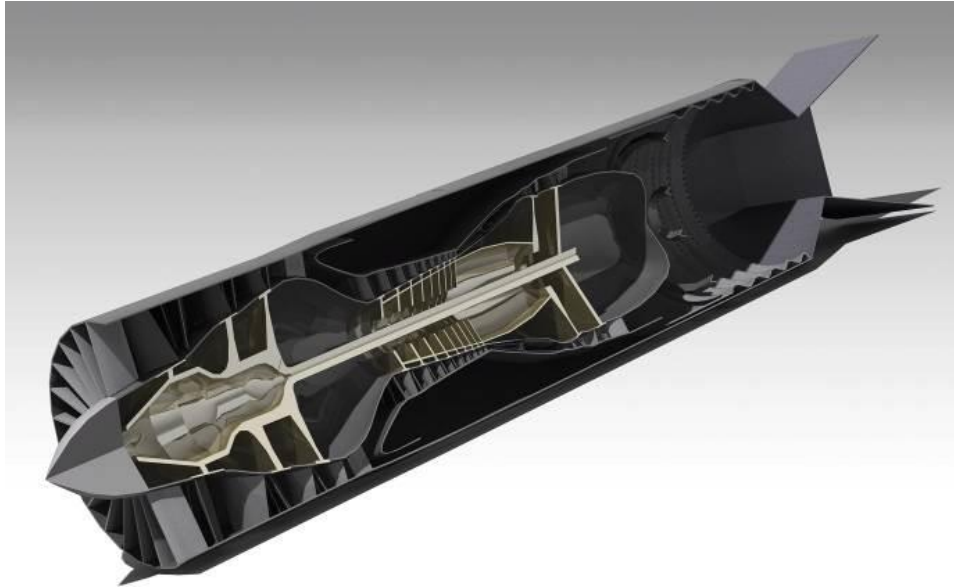


Figure 22:TJ-1 Cut-Away View

Acknowledgement

The authors gratefully acknowledge the sponsorship of Turkish Engine Industries (TEI) for the AIAA Aeroengine Design Competition.

References

- [1] I. Halliwell, "An Engine with High Power Extraction Potential for a Half Scale Model of a Joint Strike Fighter", AIAA, August 2011.
- [2] R. Whitford, "Design for Air Combat", Jane's, London, 1987.
- [3] K. Oswatich, "Pressure Recovery in Missiles with Reaction Propulsion at High Supersonic Speeds", NACA, TM1140, 1947.
- [4] P. Walsh and P. Fletcher, "Gas Turbine Performance", Oxford: Blackwell Science, 2004.
- [5] J. Mattingly, "Elements of Propulsion", American Institute of Aeronautics and Astronautics, Reston, VA, 2006.
- [6] D. Raymer, "Aircraft Design", Washington, D.C., 1992.
- [7] T. Moffitt, "Design and Cold-Air Test of Single-Stage Uncooled Core Turbine with High Work Output", TP-1680 NASA Technical Report, 1980.
- [8] J. Mattingly, W. Heiser and D. Pratt, "Aircraft Engine Design", American Institute of Aeronautics and Astronautics, Reston, VA, 2002.
- [9] E. Bachelet, "High Temperature Materials for Power Engineering Part 2", Kluwer Academic Publishers, Netherlands, 1990.
- [10] E. Gambell, D. Terrell and R. de Francesco, "Nozzle Selection and Design Criteria", 40th AIAA/ASME/SAE/ASEE Joint Propulsion Conference and Exhibit, AIAA 2004-3923, July 2004.